Goto *et al. Earth, Planets and Space* (2017) 69:26
DOI 10.1186/s40623-017-0603-9

Earth, Planets and Space

LETTER Open Access

Geomorphic features of surface ruptures associated with the 2016 Kumamoto earthquake in and around the downtown of Kumamoto City, and implications on triggered slip along active faults

Hideaki Goto[1*], Hiroyuki Tsutsumi[2], Shinji Toda[3] and Yasuhiro Kumahara[4]

Abstract

The ~30-km-long surface ruptures associated with the M_w 7.0 (M_j 7.3) earthquake at 01:25 JST on April 16 in Kumamoto Prefecture appeared along the previously mapped ~100-km-long active fault called the Futagawa-Hinagu fault zone (FHFZ). The surface ruptures appeared to have extended further west out of the main FHFZ into the Kumamoto Plain. Although InSAR analysis by Geospatial Information Authority of Japan (GSI) indicated coseismic surface deformation in and around the downtown of Kumamoto City, the surface ruptures have not been clearly mapped in the central part of the Kumamoto Plain, and whether there are other active faults other than the Futagawa fault in the Kumamoto Plain remained unclear. We produced topographical stereo images (anaglyph) from 5-m-mesh digital elevation model of GSI, which was generated from light detection and ranging data. We interpreted them and identified that several SW-sloping river terraces formed after the deposition of the pyroclastic flow deposits related to the latest large eruption of the Aso caldera (86.8–87.3 ka) are cut and deformed by several NW-trending flexure scarps down to the southwest. These 5.4-km-long scarps that cut across downtown Kumamoto were identified for the first time, and we name them as the Suizenji fault zone. Surface deformation such as continuous cracks, tilts, and monoclinal folding associated with the main shock of the 2016 Kumamoto earthquake was observed in the field along the fault zone. The amount of vertical deformation (~0.1 m) along this fault associated with the 2016 Kumamoto earthquake was quite small compared to the empirically calculated coseismic slip (0.5 m) based on the fault length. We thus suggest that the slip on this fault zone was triggered by the Kumamoto earthquake, but the fault zone has potential to generate an earthquake with larger slip that poses a high seismic risk in downtown Kumamoto area.

Keywords: 2016 Kumamoto earthquake, Active fault, Tectonic landform, Surface rupture, Kumamoto Plain, Suizenji fault zone, Digital elevation model

Background

The M_w 7.0 (M_j 7.3) earthquake occurred at 01:25 JST on April 16 in Kumamoto Prefecture, central Kyushu, southwest Japan, and caused severe shaking in and around the epicentral region. An ENE-to-NE-trending ~30-km-long surface rupture zone associated with the earthquake appeared along the previously mapped ~100-km-long active fault called the Futagawa-Hinagu fault zone (FHFZ) (Kumahara et al. 2016). The Futagawa fault, which represents the northeastern part of the FHFZ (Watanabe et al. 1979; Research Group for Active Tectonics in Kyushu 1989; Ikeda et al. 2001; Nakata and Imaizumi 2002), is located at the southern margin of the Kumamoto Plain (Fig. 1). In contrast, other possible active faults within the Kumamoto Plain has not

*Correspondence: hgoto@hiroshima-u.ac.jp
[1] Graduate School of Letters, Hiroshima University, Higashi-Hiroshima, Japan
Full list of author information is available at the end of the article

Springer Open

© The Author(s) 2017. This article is distributed under the terms of the Creative Commons Attribution 4.0 International License (http://creativecommons.org/licenses/by/4.0/), which permits unrestricted use, distribution, and reproduction in any medium, provided you give appropriate credit to the original author(s) and the source, provide a link to the Creative Commons license, and indicate if changes were made.

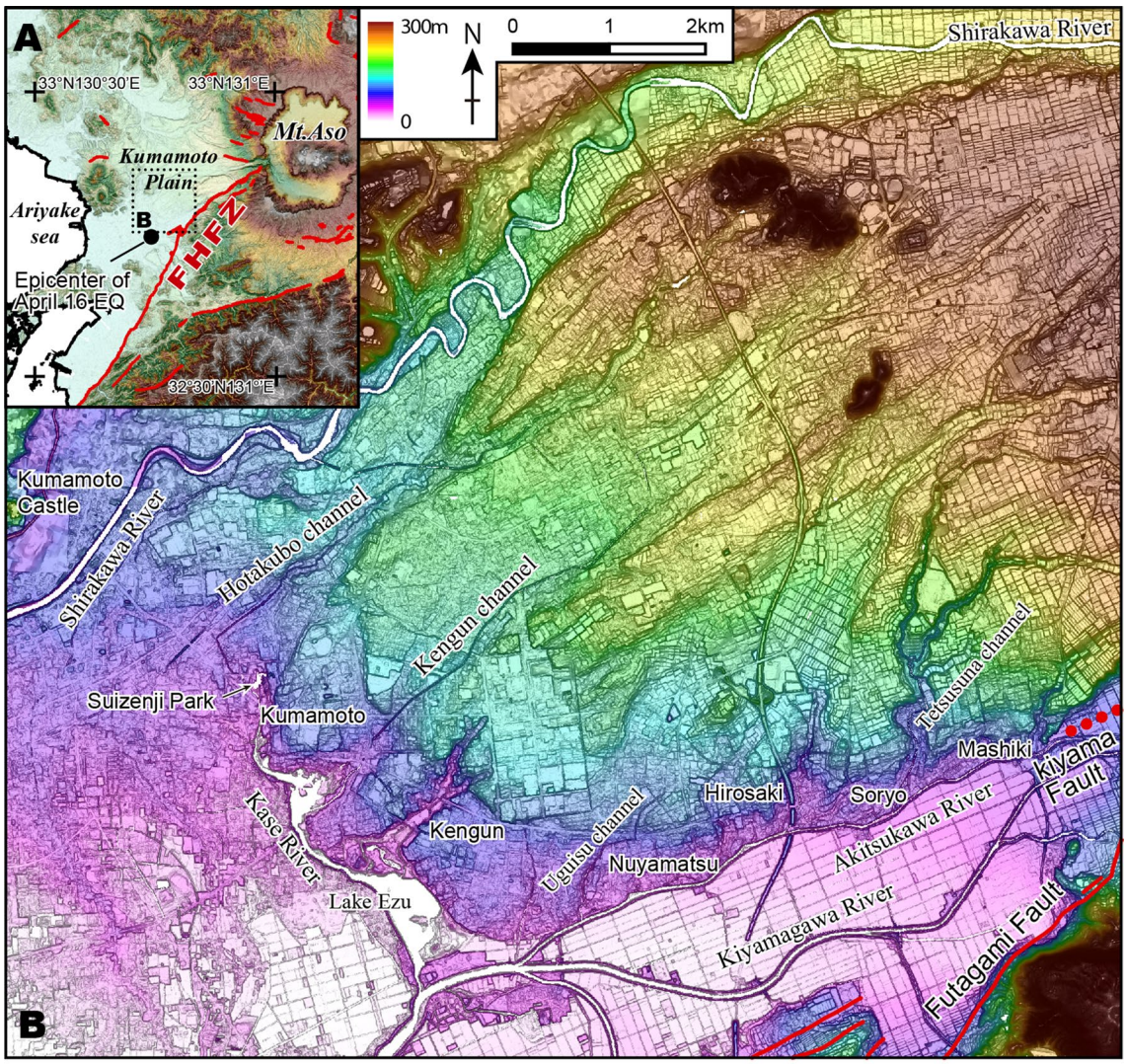

Fig. 1 *A* Active faults around the FHFZ generated the main shock of the 2016 Kumamoto earthquake sequence. The 90-m-grid digital elevation model for *shaded* relief map is after the SRTM-3 data issued by the USGS. *B* Topographical map in the central portion of Kumamoto Plain including the downtown of Kumamoto City. Active faults are after Nakata and Imaizumi (2002). The map is located in (*A*). The 5-m-grid digital elevation model for *shaded* relief map is after the Fundamental Geospatial Data issued by the GSI

been clearly mapped (Research Group for Active Faults of Japan 1991), although Watanabe et al. (1979) suggested that the E- to ENE-trending and WNW-trending faults cut the terraces of the Shirakawa River flowing westward from the Aso caldera. Numerous buildings and houses were heavily damaged in Kumamoto City, which is located in the central part of the Kumamoto Plain, although it is located far from the epicenter (Japan Meteorological Agency 2016) and the surface trace of the source fault (Kumahara et al. 2016).

In the recent years, InSAR analysis enables us to reveal the detailed and spatially comprehensive ground deformation such as faulting and tilting associated with an earthquake for an area with a few thousands square kilometers. It also often displays small displacements on the preexisting as well as unknown faults located up to ~100 km away from a source fault [e.g., 2010 El Mayor–Cucapah, California, earthquake (Wei et al. 2011)]. Nishimura et al. (2008) reported an episodic slip event on an existing shallow reverse fault that uplifted a hill by 10 cm, ~10 km away from the source fault of the 2007 Chuetsu-oki, Japan, earthquake of M_w 6.7 by analysis of InSAR data. Fujiwara et al. (2016) also found numerous small slips as interferogram fringe offsets occurred even 10 km far from the main Futagawa fault trace associated with the 2016 Kumamoto earthquake.

Here, we report our tectonic geomorphic investigations of active faults and surface ruptures which might be triggered by the 2016 Kumamoto earthquake in and around the downtown of Kumamoto City based on the interpretation of the topographical data and field survey. This study focused on the small surface ruptures along the preexisting fault that cannot be explained by the coseismic slip of a strike-slip fault as a source fault.

Methods

Our tectonic landform map was constructed mainly derived from the interpretation of the topographical images (anaglyph) (Fig. 2) produced from 5-m-mesh digital elevation model (DEM) provided by the Geospatial Information Authority of Japan (GSJ) based on light detection and ranging (LiDAR). Topographical anaglyph images, viewed with red-cyan glasses, enable us to recognize various geomorphic features (Goto and Sugito 2012). Although it is usually difficult to detect a broad deformation related to recent faulting based on conventional maps and aerial photographs, we can easily recognize such subtle deformational features on anaglyphs by increasing vertical exaggeration, especially in urban areas (Goto 2016). In this study, we also used the aerial photographs at a scale of 1:10,000 to confirm the interpretation of anaglyph images. In the field, we paid close attention to tectonic geomorphic features to map active fault traces and surface ruptures associated with the 2016 Kumamoto earthquake.

We also interviewed local people whether they have noticed any deformational features along the fault trace,

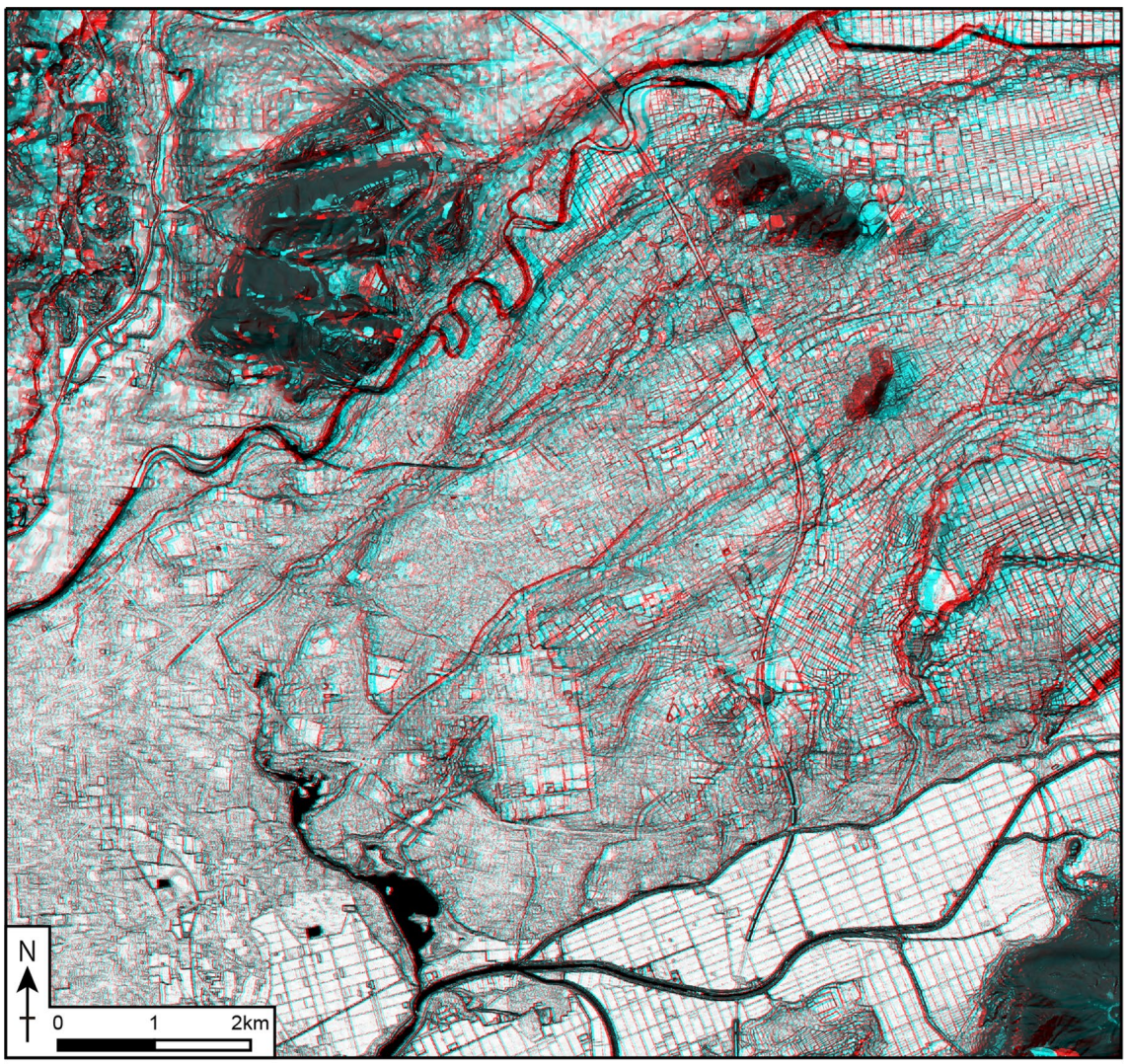

Fig. 2 Extensive area of a topographical anaglyph in the study area produced from the 5-m-grid digital elevation model of the Fundamental Geospatial Data issued by the GSI

such as surface ruptures or offsets and tilts of artificial features immediately after the large shocks on 16 April.

Geomorphic interpretation and field survey

The terrace surfaces in the study area are divided into five levels, namely Aso-4, M, L1, L2, and L3 surfaces in the descending order (Fig. 3). The Aso-4 surface is depositional surfaces of the Aso-4 pyroclastic flow deposits at about 86.8–87.3 ka during Marine Isotope Stage (MIS) 5b (Aoki 2008; Committee for Compilation of the Geological Map of Kumamoto Prefecture 2008). As the Aso-4 pyroclastic flow deposits underlie L1 and L2 gravels (Watanabe et al. 1979; Ishizaka et al. 1992), L1 and L2 surfaces were depositional terraces after the erosion of the Aso-4 deposit.

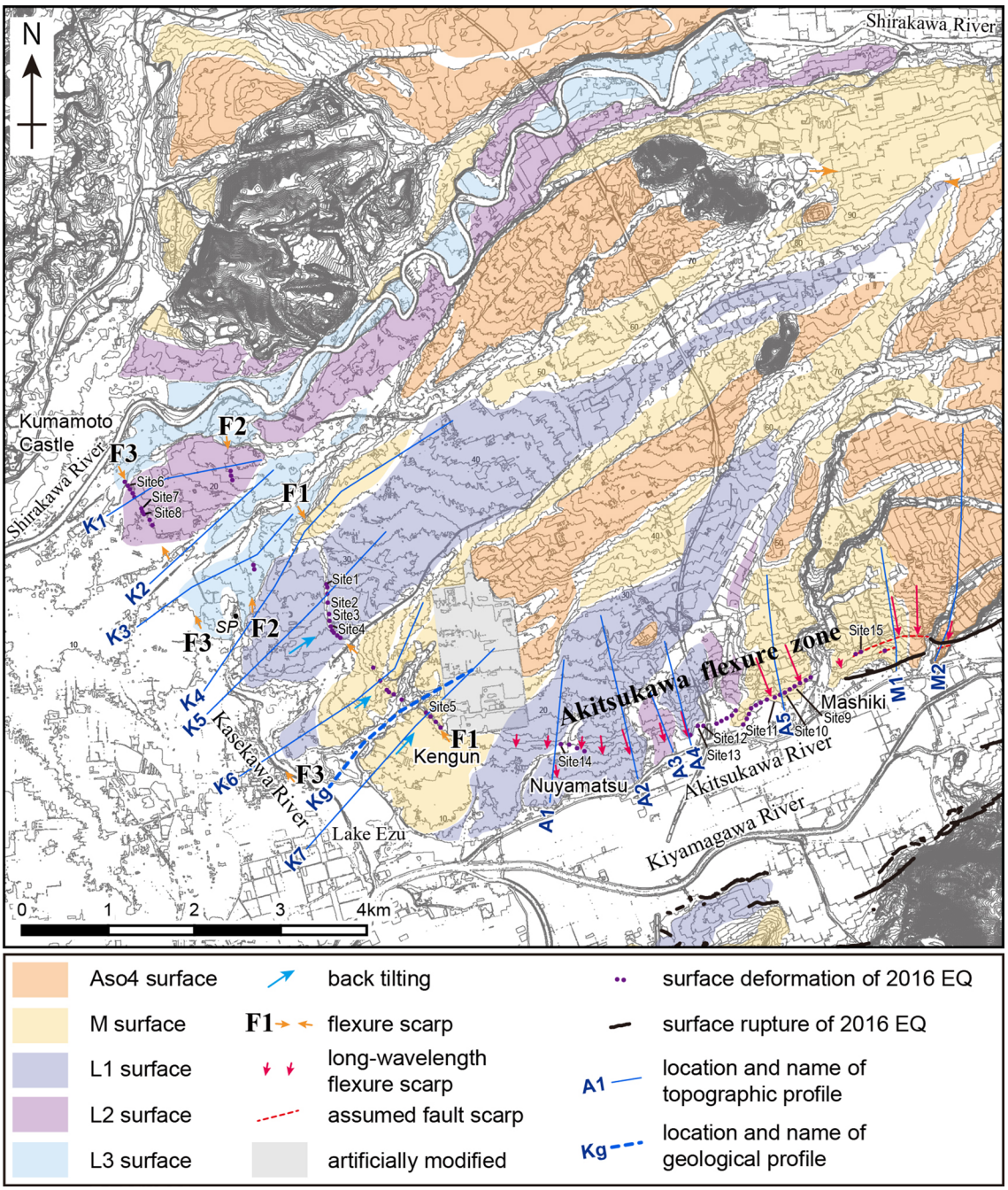

Fig. 3 Geomorphic and active fault map. The contour map is based on the 5-m-grid digital elevation model of the Fundamental Geospatial Data issued by the GSI. The trace of surface ruptures associated with 2016 Kumamoto earthquake is after Kumahara et al. (2016). *Abbreviation SP* Suizenji Jojuen Park (natural spring pond)

The Aso-4 and M surfaces can be subdivided into several surfaces, because the abandoned channels and small terrace rises are clearly observed on these surfaces. The M surfaces are distributed adjacent to the Aso-4 surface and are considered to be strath terraces of the Aso-4 surface. The L1 and L2 are well-developed surfaces in the area, while the L3 is subdivided from L2 or alluvial plain and is locally distributed. In addition, the longitudinal profiles of the L2 surfaces are steeper than those of the L1 surfaces. Thus, the development of the L1 and L2 surfaces may be closely related to the global climate change. The widespread AT tephra erupted from the Aira caldera in south Kyusyu at about 28–29 ka (Murayama et al. 1993) during MIS 3 is contained in the middle part of aeolian deposit overlying L2 gravels (Watanabe et al. 1995). Therefore, the L1 and L2 terraces were likely formed between MIS 5a and MIS 3.

Suizenji fault zone

We found the NW-trending flexure scarps down to the southwest that cut across the M, L1, and L2 terraces in the downtown of Kumamoto City based on the interpretation of the anaglyph images (Fig. 3). Three discernible subparallel fault strands (F1–F3) are called collectively as the Suizenji fault zone in this paper.

The F1 is recognized from the east of Hotakubo channel to Kengun for a length of 3 km as N- to NW-trending steep scarps on the L1 and M surfaces, which generally dips to the southwest. We interpret these steep scarps as tectonic flexure scarps, since the strike of F1 is almost perpendicular to the incised channels of the L1 and M terraces such as the Hotakubo and Kengun channels, and the slope angles and direction of the terrace surfaces are generally the same on the both sides of F1. The amounts of vertical offset on the L1 and M terraces are 6.2–7 and 8.2–9.5 m, respectively (Fig. 4). The southern part of the M and L1 surfaces on the downthrown side of F1 might be slightly tilted toward the upstream (Fig. 4, K5–7). This observation suggests that F1 may be a southwest-dipping normal fault, which we shall discuss in more details in the later Discussion section.

F2 is located ~800 m west of F1 and parallel to the northern part of F1. The NNW-trending flexure scarps of F2 cut across the L2 and L3 surfaces formed by the Shirakawa River flowing to the southwest. The amounts of vertical offset on the L2 and L3 surfaces are 3.5–4.3 and 2.7 m, respectively (Fig. 4).

The L2 surfaces are incised by the meandering Shirakawa River near the downtown of Kumamoto, suggesting an uplift of the area. At the south bank of this river, the gently sloping L2 surface is offset by the NW-trending steep scarp of F3. On the east side of the southern extension of this scarp, the L3 terraces are exceptionally well developed. The L3 terraces are separated from the alluvial plain with the NW-trending straight scarps of F3. Along the possible southern extension of F3, the L1 surfaces are also juxtaposed against the alluvial plain and wetland along the Kasegawa River and Lake Ezu gushing spring water out of the underground, which may suggest the existence of a buried fault at the southern extension of F3.

Subsurface structures derived from shallow borehole data and Bouguer anomalies indicate that the flexure scarps were formed by the buried active fault. A geological cross section derived from borehole data across F1 (Kumamoto City Waterworks Bureau 1980) shows a 10-m vertical offset of the Aso-4 pyroclastic flow deposits retrieved from all the boreholes on the both sides of the scarp (Fig. 4b). The upward convex deformation of the Aso-4 unit on the downthrown side is similar to the F1 scarp profiles of K4 and K5 in Fig. 4a, suggesting a rollover anticline associated with the SW-dipping normal fault. The amount of the vertical offset of the Aso-4 deposits, more than 10 m, is evidently larger than that of the M1 surfaces, which may indicate cumulative fault slip as a result of repeating movements. The long-term vertical slip rate of the F1 is estimated to be around 0.1 mm/year, based on the amount of the vertical offset of the Aso-4 deposits and its age.

In addition to the geomorphic and surface stratigraphic analyses, one of the distinctive subsurface structural boundaries estimated from Bouguer anomalies (Matsumoto et al. 2016) is consistent with the Suizenji fault zone and the Akitsugawa flexure zone.

Akitsugawaa flexure zone

We also found the ENE-trending long-wavelength flexure scarps along the northern margin of the alluvial plain of the Kiyamagawa River (Fig. 3). We name them the Akitsugawa flexure zone. The steep slope zone continues across the terraces from the east of Mashiki to the west of Nuyamatsu. The amounts of vertical offset on the M, L1, and L2 surfaces are 6, 3–4, and 2 m, respectively (Fig. 5). The widths of the steeply sloping zone on the M, L2, and L2 surfaces are about 400–500, 100–300, and 200 m, respectively, and are considerably larger compared to those along the Suizenji fault zone. We suggest that this surface deformation has been formed by a buried active fault.

The Kiyama fault is believed to be a buried active fault on the eastern extension of the Akitsugawa flexure zone, based on the subsurface distribution of the Tokawa lava (Watanabe et al. 1979). The Akitsugawa flexure zone may be connected to the Kiyama fault at seismogenic depth and form a single active fault system.

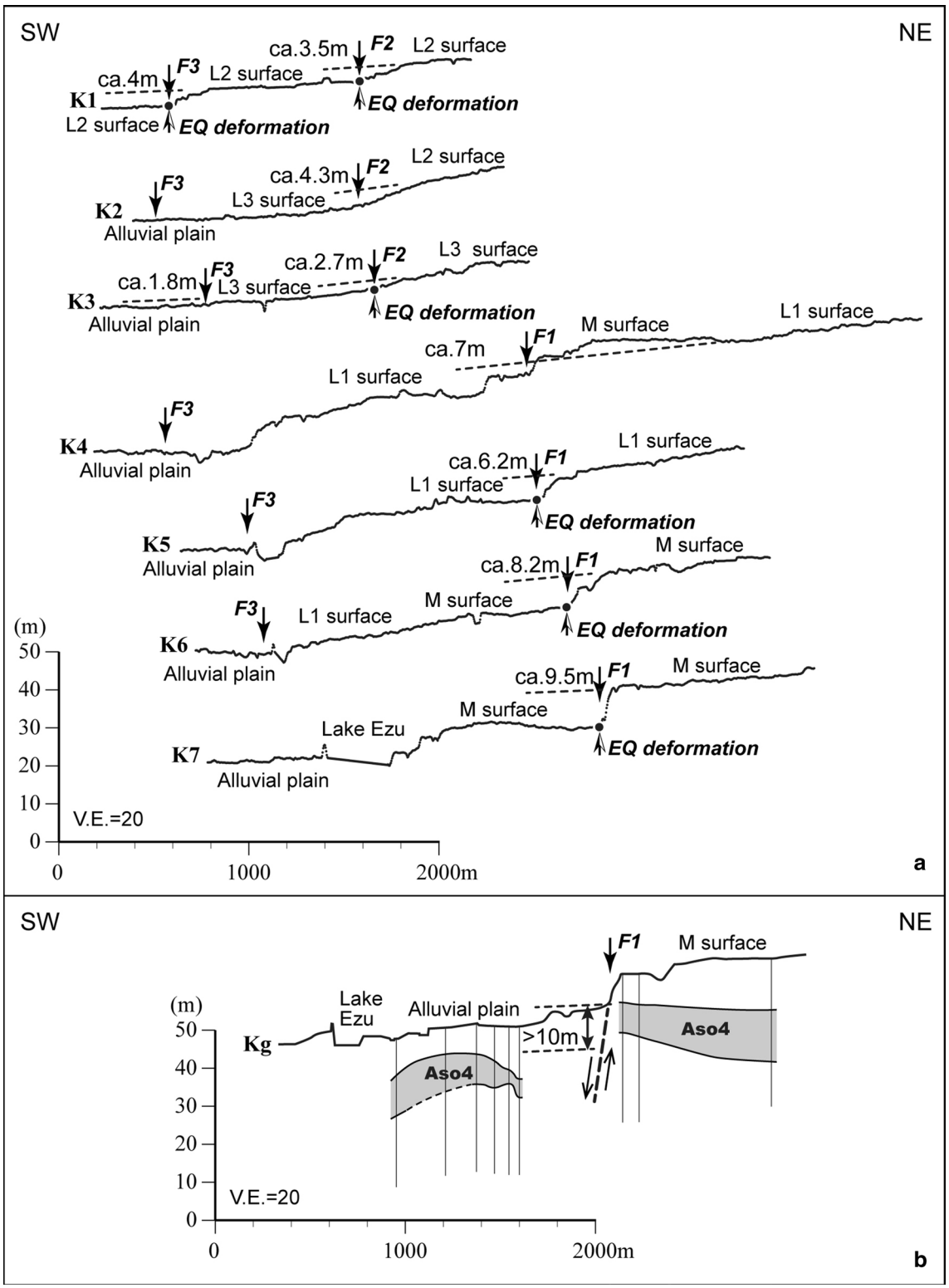

Fig. 4 **a** Topographical profiles across the Suizenji fault zone based on the DEM. The *measured lines* are shown in Fig. 3. **b** A geological cross section derived from borehole data across F1. The location of section is shown in Fig. 3

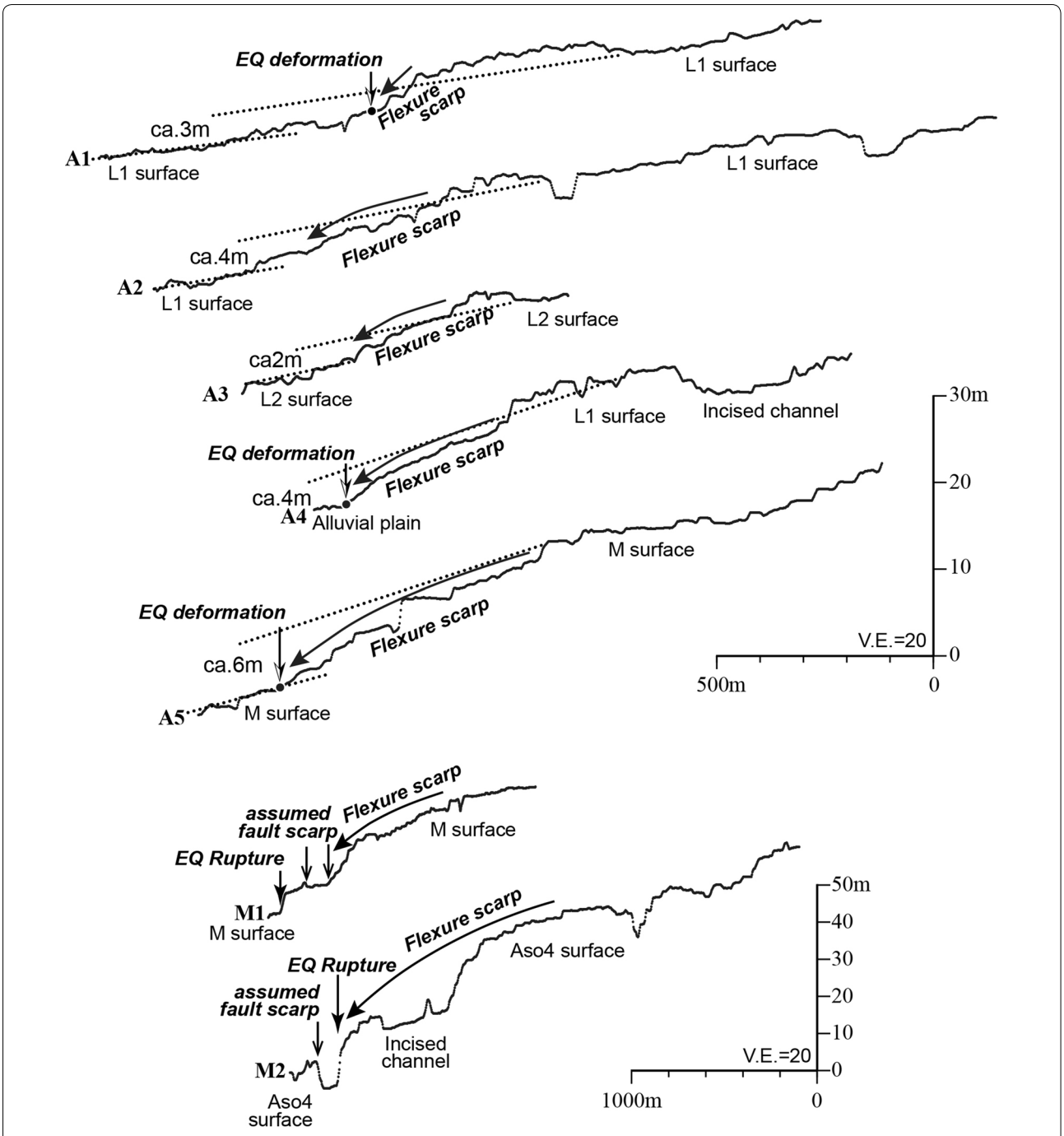

Fig. 5 Topographical profiles across the Akitsugawa flexure zone based on the DEM. The *measured lines* are shown in Fig. 3

Surface ruptures of the 2016 earthquake

Surface ruptures associated with the 2016 earthquake appeared along the Futagawa fault zone on the southern margin of the alluvial plain of the Kiyama River (Kumahara et al. 2016). A part of the rupture zone extends into the downtown of Mashiki on the northern margin of the plain and nearly reaches the eastern extension of the Akitsugawa flexure zone. Interpretation of the InSAR image of GSI (2016a) and Fujiwara et al. (2016) led us to recognize ~10-cm-scale coseismic offset or deformation along Suizenji fault zone and its extension (Fig. 6). Motivated by the image, we conducted field surveys to identify whether surface deformation such as open cracks, tilts, and shortenings appeared on the surface along the Suizenji fault zone.

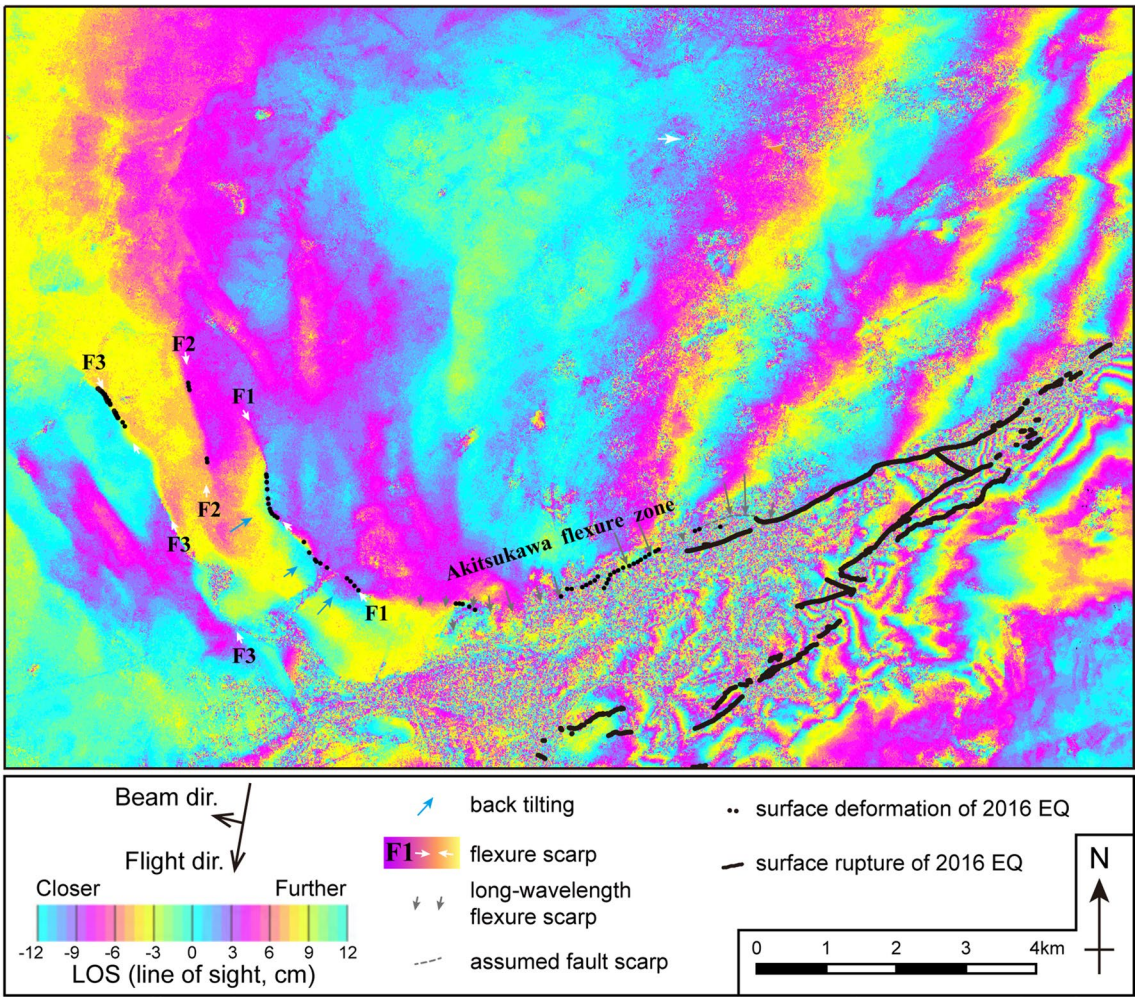

Fig. 6 Distribution of active faults and surface deformation associated with 2016 Kumamoto earthquake dropped over the InSAR deformation map, descending interferograms computed from ALOS-2/PALSAR-2 images of March 7, 2016, and April 18, 2016 (Geospatial Information Authority of Japan 2016a). The trace of surface ruptures associated with 2016 Kumamoto earthquake is after Kumahara et al. (2016)

In many places along F1, a series of continuous open cracks were observed on the artificial features like asphalt roads and retaining walls. Buckling of asphalt was also found at the base of scarps at several places (Fig. 7a–f). The indoor pool of the Kumamoto Technical High School constructed on the flexure scarp was tilted to the west by 8 cm based on the height difference of the water surface and upper edge of the pool (Fig. 7b). According to the local residence, these features along F1 appeared in the midnight of 16 April at the time of the main shock of the 2016 Kumamoto earthquake. Fault-related deformation like open cracks was found at only a few places along F2, suggesting that the amount of offset was smaller than that along the F1.

Along the northern part of F3, continuous surface deformation including right-stepping en echelon open cracks and 0.5-cm left-lateral offset of the concrete block wall were observed (Fig. 7g–j). Houses and concrete buildings standing between the visible deformation features like open cracks on asphalt roads were heavily damaged, implying that the structural basements might be also deformed by faulting. According to the local residence, these features were found in the morning of 16 April after the main shock of the 2016 Kumamoto earthquake.

Small deformation like continuous cracks and buckling was also observed near the base of flexure scarp of the Akitsugawa flexure zone at several places (Fig. 7k–q). From the west of downtown Mashiki, where surface fault ruptures evidently emerged (Kumahara et al. 2016) to Hirosaki, Mashiki town, the continuous cracks and buckling of asphalt were intermittently extended (Fig. 3). A five-storied reinforced concrete building just on the continuous cracks was tilted at Shoryo in Mashiki town (Fig. 7k).

Fig. 7 Snapshots of surface deformation along the Suizenji fault zone (*site 1–8*) and the Akitsukawa flexure zone (*site 9–15*). The localities of the site are shown in Fig. 3

Discussion

Our interviews with the local residents enable us to conclude that the series of minor ruptures on the Suizenji fault zone and the Akitsugawa flexure zone were the products of the 2016 Kumamoto main shock. However, regarding the relation between the 2016 ruptures and the preexisting fault zone, one could raise critical questions about whether these slips were indeed triggered by the coseismic deformation, and/or whether they occurred only on the shallow part of the fault zones, and/or whether the Suizenji fault still keeps stress unreleased at seismogenic depth.

To seek better answers to the questions, here we have plotted aftershocks and focal mechanisms with the 2016 surface breaks (Fig. 8a, b). A NW-trending cluster of numerous shallow aftershocks (red dots in Fig. 8a) mostly extended to the northwest from the Suizenji fault zone, indicating the after slip might have occurred at least down to a few kilometers. A majority of the aftershock mechanisms plotted near the Suizenji fault zone are NW-striking normal faults, which is consistent with our geomorphic estimate of slip sense along the Suizenji fault zone.

To confirm these shallow slip and aftershocks were indeed triggered by the 2016 Kumamoto main shock, we calculated static Coulomb stress change (ΔCFF, e.g., King et al. 1994) in an elastic half-space of Okada (1992) with Poisson's ratio of 0.25 and Young's modulus of 80 GPa. We used a source fault model of GSI (2016b) and then resolved ΔCFF on NW-trending normal faults and NW-trending reverse faults (Fig. 8c, d). We found that the normal faults around the Suizenji fault zone were favorably oriented for failure due to the 2016 Kumamoto earthquake, and the NW–SE stretched stressed lobe is totally consistent with the trend of the minor ruptures on the Suizenji fault zones (Fig. 8c). In contrast, the thrust faults in the Suizenji area are calculated to have moved farther away from failure (Fig. 8d), which may deny a possibility that the Suizenji fault zone is an east-dipping reverse fault.

Remotely triggered small amounts of slip other than our study area are also found by the InSAR analysis (Fujiwara et al. 2016). In the northwest of the outer rim of Aso caldera, in particular, slip on numerous short EW-trending lineaments, some of which are previously mapped as active faults, contributed to develop low valleys by their sawtooth normal faulting displacements. These peripheral small faults, responded to the movement of the major fault movement, may provide us a clue to understand low slip rate and short active faults ubiquitously exist. No aftershocks beneath the northwest of the outer rim of Aso caldera also support the idea that these faults are always passively moved for adjusting local stress disturbed by major earthquakes nearby.

On the other hand, we suspect the Suizenji fault zone has a potential to generate its own earthquake. Adopting the empirical relation of fault length and maximum displacement by Matsuda (1975), ~6-km-long Suizenji fault zone could have brought ~0.5-m vertical displacement. However, maximum vertical slip measured was ~0.1 m that might be a tiny fraction of its potential slip. Thus, we do not believe that these triggered slips completely released stress that the Suizenji fault has stored. Instead, they are now brought closer to failure (Fig. 8c) if stress at the seismogenic depth is indeed accumulated. Furthermore, the elongated shallow seismic cluster implies that the subsurface fault structure might be further extended to the northwest as inferred from the Bouguer anomalies (Matsumoto et al. 2016), which may have a capability to produce an earthquake as large as $M \sim 6.5$. It may be a part of the post-Kumamoto earthquake hazard as well as the widespread off-fault aftershocks beneath the entire Kumamoto Plain.

Concluding remarks

Several NW-trending and SW-facing flexure scarps (the Suizenji fault zone) were newly identified for a length of 5.4 km departed from the main coseismic Futagawa surface fault trace in the downtown of Kumamoto City based on the interpretation of topographical stereo images (anaglyph) produced from 5-m-mesh DEM of GSI, which was generated from LiDAR data. Up to 10-cm vertical offset of surface deformation such as cracks, tilts, and buckling associated with the main shock of the 2016 Kumamoto earthquake were observed along the Suizenji fault zone. Our field observations are consistent with the interpretation of the Interferometric SAR image (GSI 2016) processed using ALOS-2/PALSAR-2 data spanning the main shock of the Kumamoto earthquake (Fujiwara et al. 2016). The ENE-trending and SE-facing long-wavelength flexure scarps (Akitsugawa flexure zone) were also identified on the anaglyph images in the area between the apparent surface ruptures of the 2016 Kumamoto earthquake and the Suizenji fault zone. The surface deformation along this zone seems to have been caused by the buried fault beneath the Akitsugawa flexure zone. Because the amount of offset (~0.1 m) observed in the field and on the Interferometric SAR image is considerably smaller than the slip (0.5 m) empirically calculated from the fault length, it is likely that the 2016 Kumamoto earthquake only caused small amounts of triggered slip on this fault zone. The risk of another large earthquake from these structures still remains high in the downtown of Kumamoto, although the city is located a few km away from the Futagawa-Hinagu fault zone (FHFZ).

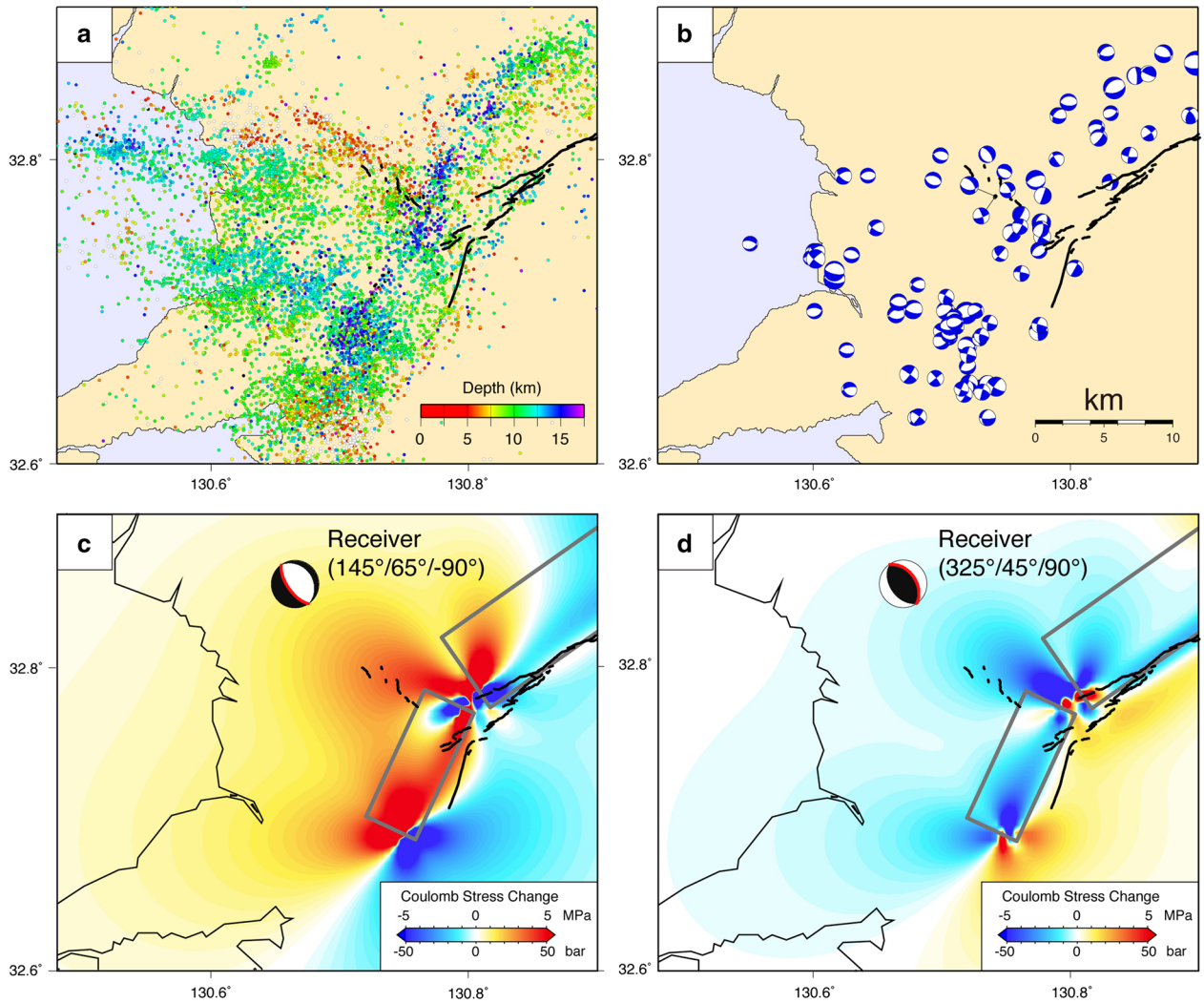

Fig. 8 Spatial relations of the NW-trending minor surface ruptures with aftershocks, focal mechanisms, and stress imparted from the Kumamoto main shock. **a** Aftershocks from the Japan Meteorological Agency catalog until September 18, 2016. **b** Focal mechanisms of the larger aftershocks determined from National Research Institute for Earth Science and Disaster Resilience (2016). **c** Coulomb stress change resolved onto NW-striking normal faults. **d** Coulomb stress change resolved onto NW-striking thrust faults. In both **c** and **d**, the source fault model of the Geospatial Information Authority of Japan (2016a) as *gray rectangular* is used for the stress calculation with apparent coefficient of friction 0.4 at a depth of 2.5 km. Receiver fault that Coulomb stress is resolved is shown as the *red line* on the *beach ball* and in the *parentheses* (strike/dip/rake) on *each panel*

Authors' contributions
HG planed and conducted all the fieldwork and drew the figures. HG wrote the text with HT and ST. HT and YK discussed the interpretation of tectonic landform with HG and did the fieldwork. ST calculated stress change in Fig. 8. ST and YK discussed the interpretation of InSAR image and distribution of aftershock with HG. All authors read and approved the final manuscript.

Author details
[1] Graduate School of Letters, Hiroshima University, Higashi-Hiroshima, Japan. [2] Graduate School of Science, Kyoto University, Kyoto, Japan. [3] International Research Institute of Disaster Science, Tohoku University, Sendai, Japan. [4] Graduate School of Education, Hiroshima University, Higashi-Hiroshima, Japan.

Acknowledgements
This work was partly supported by MEXT KAKENHI Grant Numbers 16H06298 and 16K01221. We thank staffs of Kumamoto Technical High School, who allowed us to conduct our fieldwork inside the school property. We are grateful to Dr. Hisao Kondo and Dr. Jian-Cheng Lee for providing valuable comments and suggestions, which helped us in progressing our study and improving the manuscript.

Competing interests
The authors declare that they have no competing interests.

Received: 31 July 2016 Accepted: 14 January 2017
Published online: 02 February 2017

References

Aoki K (2008) Revised age and distribution of ca. 87 ka Aso-4 tephra based on new evidence from the northwest Pacific Ocean. Quat Int 178:100–118

Committee for Compilation of the Geological Map of Kumamoto Prefecture (2008) 1: 100,000 geological map of Kumamoto Prefecture. Kumamoto Geotechnical Consultant Association Corp (**in Japanese**)

Fujiwara S, Yarai H, Kobayashi T, Morishita Y, Nakano T, Miyahara B, Nakai H, Miura Y, Ueshiba H, Kakiage Y, Une H (2016) Small-displacement linear surface ruptures of the 2016 Kumamoto earthquake sequence detected by ALOS-2 SAR interferometry. Earth Planets Space 68:160. doi:10.1186/s40623-016-0534-x

Geospatial Information Authority of Japan (2016a) Detection of crustal movement by ALOS-2 InSAR. http://www.gsi.go.jp/BOUSAI/H27-kumamoto-earthquake-index.html#3. Accessed 7 July 2016 (**in Japanese**)

Geospatial Information Authority of Japan (2016b) Provisional source fault model of the 2016 Kumamoto earthquake Accessed 7 September 2016. http://www.gsi.go.jp/common/000140781.pdf (**in Japanese**)

Goto H (2016) Extensive area map of topographic anaglyphs covering inland and seafloor from detailed digital elevation model for identifying broad tectonic deformation. In: Kamae K (ed) Earthquakes, Tsunamis and nuclear risks: prediction and assessment beyond the Fukushima accident. Springer, Japan, pp 65–74. http://link.springer.com/chapter/10.1007%2F978-4-431-55822-4_5

Goto H, Sugito N (2012) Fault geomorphology interpreted using stereoscopic images; produced from digital elevation models. E-J GEO 7:197–213 **(in Japanese with abstract in English)**

Ikeda Y, Chida N, Nakata T, Kaneda H, Tajikara M, Takazawa S (2001) 1:25,000-scale active fault map in urban area "Kumamoto". Technical report of the Geographical Survey Institute, Ibaraki, D1-No. 388 (**in Japanese**)

Ishizaka S, Watanabe K, Takada H (1992) Subsidence rate of the underground quaternary system for the past 150,000 years in the Kumamoto Plain, Kyushu, Japan. Quat Res 31:91–99 **(in Japanese with abstract in English)**

Japan Meteorological Agency (2016) CMT solutions of the earthquake occurred in April, 2016. http://www.data.jma.go.jp/svd/eqev/data/mech/cmt/cmt201604.html. Accessed 7 July 2016 (**in Japanese**)

King GCP, Stein RS, Lin J (1994) Static stress changes and the triggering of earthquakes. Bull Seismol Soc Am 84:935–953

Kumahara Y, Goto H, Nakata T, Ishiguro S, Ishimura D, Ishiyama T, Okada S, Kagohara K, Kashihara S, Kaneda H, Sugito N, Suzuki Y, Takenami D, Tanaka K, Tanaka T, Tsutsumi H, Toda S, Hirouchi D, Matsuta N, Moriki H, Yoshida H, Watanabe M (2016) Distribution of surface rupture associated with the 2016 Kumamoto earthquake and its significance. Japan Geoscience Union Meeting 2016, MIS34-05

Kumamoto City Waterworks Bureau (1980) The underground water in and around Kumamoto city. Kumamoto City Waterworks Bureau (**in Japanese**)

Matsuda T (1975) Magnitude and recurrence interval of earthquakes from a fault. J Seismol Soc Jpn 28:269–283 **(in Japanese with abstract in English)**

Matsumoto N, Yoshihiro H, Sawada A (2016) Continuity, segmentation and faulting type of active fault zones of the 2016 Kumamoto earthquake inferred from analyses of a gravity gradient tensor. Earth Planets Space 68:167. doi:10.1186/s40623-016-0541-y

Murayama M, Matsumoto E, Nakamura T, Okamura M, Yasuda H, Taira A (1993) Reexamination of the eruption age of Aira-Tn (AT) obtained from a piston core off Shikoku; determined by AMS 14C dating of planktonic foraminifera. J Geol Soc Jpn 99:787–798 **(in Japanese with abstract in English)**

Nakata T, Imaizumi T (eds) (2002) Digital active fault map of Japan. University of Tokyo Press, Tokyo **(in Japanese with abstract in English)**

National Research Institute for Earth Science and Disaster Resilience (2016) Earthquake mechanism information by broadband seismic network (F-net). http://www.fnet.bosai.go.jp/event/joho.php?LANG=en

Nishimura T, Tobita M, Yarai H, Amagai T, Fujiwara M, Une H, Koarai M (2008) Episodic growth of fault-related fold in northern Japan observed by SAR interferometry. Geophys Res Lett. doi:10.1029/2008GL034337

Okada Y (1992) Internal deformation due to shear and tensile faults in a half-space. Bull Seismol Soc Am 82:1018–1040

Research Group for Active Faults of Japan (1991) Active faults in Japan: sheet maps and inventories, revised edn. University of Tokyo Press, Tokyo **(in Japanese with abstract in English)**

Research Group for Active Tectonics in Kyushu (1989) Active Tectonics in Kyushu. University of Tokyo Press, Tokyo **(in Japanese with abstract in English)**

Watanabe K, Momikura K, Tsuruta K (1979) Active faults and parasitic eruption centers on the west flank of Aso caldera, Japan. Quat Res 18:89–101 **(in Japanese with abstract in English)**

Watanabe K, Takada H, Okabe R, Nishida A (1995) Stratigraphic relation between fluvial terrace deposits and widespread tephra beds in the middle reaches of the Sirakawa, Kumamoto Prefecture, Japan. Memoirs of the Faculty of Education. Kumamoto University. Nat Sci 44:15–22 **(in Japanese with abstract in English)**

Wei M, Sandwell D, Fialko Y, Bilham R (2011) Slip on faults in the Imperial Valley triggered by the 4 April 2010 M_w 7.2 El Mayor–Cucapah earthquake revealed by InSAR. Geophys Res Lett. doi:10.1029/2010GL045235

Submit your manuscript to a SpringerOpen journal and benefit from:

- ► Convenient online submission
- ► Rigorous peer review
- ► Immediate publication on acceptance
- ► Open access: articles freely available online
- ► High visibility within the field
- ► Retaining the copyright to your article

Submit your next manuscript at ► springeropen.com